Journal of Hazardous Materials 171 (2009) 294–300

Contents lists available at ScienceDirect

Journal of Hazardous Materials

journal homepage: www.elsevier.com/locate/jhazmat

Photo degradation of methyl orange by attapulgite–SnO_2–TiO_2 nanocomposites

Lili Zhang[a,b,*], Fujian Lv[a], Weiguang Zhang[a], Rongqing Li[a], Hui Zhong[a], Yijiang Zhao[a], Yu Zhang[a], Xin Wang[b,**]

[a] Jiangsu Key Laboratory for Chemistry of Low-Dimensional Materials, Huaiyin Normal University, Huai'an 223300, China
[b] Materials Chemistry Laboratory, Nanjing University of Science and Technology, Nanjing 210097, China

ARTICLE INFO

Article history:
Received 23 November 2008
Received in revised form 6 May 2009
Accepted 29 May 2009
Available online 7 June 2009

Keywords:
Methyl orange
Photo degradation
Attapulgite
Sol–gel technique
SnO_2–TiO_2

ABSTRACT

Photocatalytic removal of methyl orange under ultraviolet radiation has been studied using attapulgite (ATT) composites, which were synthesized by depositing SnO_2–TiO_2 hybrid oxides on the surface of ATT to form a composite photocatalyst (denoted ATT–SnO_2–TiO_2) using an *in situ* sol–gel technique. Results showed that SnO_2–TiO_2 nanocomposite particles with average size of about 10 nm were loaded successfully on to the surface of ATT fibers and were widely dispersed. Correspondingly, the photocatalytic activity of ATT was improved significantly by loading SnO_2–TiO_2. The photoactivity of the composite photocatalyst decreased in the sequence ATT–SnO_2–TiO_2 > ATT–SnO_2 > ATT–TiO_2 > ATT. In order to achieve the best photocatalyst, the molar ratio of SnO_2 and TiO_2 in the ATT–SnO_2–TiO_2 composites was adjusted to give a series with proportions $r = n_{Ti}/(n_{Ti} + n_{Sn}) = 0.0, 0.25, 0.33, 0.50, 0.67, 0.75, 0.80, 0.82, 0.86, 1.0$. Results indicated that the proportion of SnO_2 and TiO_2 had a critical effect on the photocatalytic activity, which increased as the content of TiO_2 increased to $r \leq 0.82$ and decreased when $r > 0.82$. The highest degradation rate of methyl orange was 99% within 30 min obtained by using ATT–SnO_2–TiO_2 with $r = 0.82$. The repeated use of the composite photocatalyst was also confirmed.

1. Introduction

Recently, the application of solar energy conversion to environmental cleanup has been one of the most active research areas in photocatalysis [1–4]. The use of titanium dioxide for advanced water treatment and water purification processes has attracted growing attention since 1972 [5]. It is well known that the photocatalytic activity of TiO_2 usually depends on the ratio of the transfer rate of surface charge carriers from the interior to the surface and the recombination rate of photo-generated charge carriers. If the recombination occurs too rapidly (<0.1 ns), there is not enough time for other chemical reactions to take place [6]. It is therefore important to decrease the recombination of photogenerated charge carriers. Coupling TiO_2 with other semiconductors has been widely studied and the corresponding composite photocatalysts have been proved to perform well because of their high quantum yield [7–9]. For example, Tada [10–13] and Vinodgopal and Kamat [14] conducted systematic research on the use of SnO_2 as a coupled semiconductor and confirmed that the photogenerated electrons in the SnO_2–TiO_2 system can accumulate on the SnO_2 and the photogenerated holes can accumulate on the TiO_2 because of the formation of a heterojunction at the SnO_2–TiO_2 interface. This can result in a lower recombination rate of photogenerated charge carriers, higher quantum efficiency and better photocatalytic activity.

But all of these photocatalysts have the same problems, including their fixation, diffusion and recycling. It has been reported that the support-based photocatalysts, which can adsorb and concentrate the reactants but still allow the latter to diffuse from the adsorption site to the photocatalyst surface, were quite efficient in improving the degradation rate of the pollutants [15–17]. In addition, supported catalysis has been awarded the status of "green" chemistry because it allows easy separation of the products and permits the recycling and reuse of the catalysts, giving both operational and economical advantages [18]. For example, hybrid photocatalysts consisting of TiO_2 and activated carbon (AC) have been shown to exhibit a higher rate of degradation of several organic compounds compared with that of unmodified TiO_2 [16,17]. Another promising material for these systems is clay or a clay-based matrix, which is chemically inert, resistant to deterioration, commercially available in large quantities and has many industrial, catalytic and environmental applications [19–25].

Attapulgite (ATT, or palygorskite, as it often called), a species of hydrated magnesium aluminum silicate non-metallic mineral [$(H_2O)_4(Mg,Al,Fe)_5(OH)_2Si_8O_{20}\cdot 4H_2O$] with commonly a lath

* Corresponding author at: Jiangsu Key Laboratory for Chemistry of Low-Dimensional Materials, Huaiyin Teachers College, Changjiang West road 111#, Huai'an 223300, China. Tel.: +86 517 83525312; fax: +86 517 83525311.
** Corresponding author. Tel.: +86 517 83525312; fax: +86 517 83525311.
E-mail address: Zhanglily800@yahoo.com.cn (L. Zhang).

0304-3894/$ – see front matter © 2009 Elsevier B.V. All rights reserved.
doi:10.1016/j.jhazmat.2009.05.140

or fibrous morphology, is characterized by a porous crystalline structure containing tetrahedral layers alloyed together along longitudinal sideline chains [26]. Due to its unique structure and considerable textual properties, natural ATT has been widely used as adsorbents, adhesives, catalysts and as catalyst supports [27–33]. Zhao [29,32] prepared silver and copper modified ATT/TiO_2 photocatalysts by a hydrolysis method, which exhibited much higher activity than that of the pure TiO_2 for the degradation of methylene blue. Lei et al. [18] prepared ATT-supported Sn catalysts for the catalytic oxidation of cyclic ketones and acyclic ketones by hydrogen peroxide, affording the corresponding lactones or esters with selectivity of 90–99%. In this work, we have used ATT as the support for the SnO_2–TiO_2 hybrid oxide for the photodecomposition of methyl orange. The resultant ATT–SnO_2–TiO_2 photocatalysts showed interesting photocatalytic activity, suggesting that this ATT–SnO_2–TiO_2 system could be a potential environmental catalyst system.

2. Materials and methods

2.1. Preparation of photocatalysts

ATT, with an average particle size of 200-mesh, was provided by Jiangsu ATP Co. Ltd. Its chemical composition was 58.23–66.30% SiO_2, 10.50–11.90% Al_2O_3, 8.10–12.65% MgO, 5.80–6.51% Fe_2O_3, 0.76–1.10% TiO_2, 0.008–0.15% Mn_2O_3, 0.68–0.91% K_2O, 0.29–4.15% CaO and 0.02–0.13% MnO. Tetrabutyl titanate ($Ti(OBu)_4$) and hydrous sub-stannic chloride ($SnCl_2{\cdot}2H_2O$) were used as precursors for titania and stannic oxide, respectively. The mass ratio of ATT and SnO_2 in the later composite photocatalyst was fixed at about 10/3. In order to adjust the proportions of SnO_2 and TiO_2 in ATT–SnO_2–TiO_2, the values of $r = n_{Ti}/(n_{Ti} + n_{Sn})$ were set to 0.0, 0.25, 0.33, 0.50, 0.67, 0.75, 0.80, 0.82, 0.86, 1.0, where n_{Ti} and n_{Sn} represent the molar numbers of SnO_2 and TiO_2, respectively. $r = 0.0$ corresponds to ATT–SnO_2, whereas $r = 1.0$ corresponds to ATT–TiO_2.

The preparation procedure for the ATT–SnO_2–TiO_2 nanocomposites is illustrated in the flowchart of Fig. 1. In order to reduce the time required for the overall synthetic process, the first step is the simple purification of ATT. Raw ATT (5 g) was dispersed in 100mL distilled water in an ultrasonic bath for 0.5 h, then the nether sand and large stones were removed. This produced a homogeneous ATT suspension which was used directly in the later modification section without further acid activation. Secondly, appropriate amounts of $SnCl_2{\cdot}2H_2O$ (e.g. $m = 2.25$ g for $r = 0.82$) were dissolved in 15 mL dense hydrochloric acid and added slowly to the upper ATT suspension. The mixture was thoroughly stirred using a magnetic mixer for 0.5 h. Then concentrated ammonia was added to make $SnCl_2$ hydrolyze *in situ* and deposit nanosized $Sn(OH)_2$ on to the surface of the ATT. The ultimate pH value of the suspension was adjusted to 6–7 to ensure the complete hydrolysis of $SnCl_2$. After aging for 4 h, the mixture was filtered and washed with distilled water. The resulting solid was dried at 80 °C for 4 h and subsequently calcined at 300 °C for 4 h and denoted as ATT–SnO_2. Thirdly, a given amount of $Ti(OBu)_4$ (e.g. $m = 17.00$ g for $r = 0.82$) was added to the ATT–SnO_2 powders whilst milling and then 100 mL distilled water was added drop by drop to let the $Ti(OBu)_4$ hydrolyze *in situ* to deposit $Ti(OH)_4$ on to the surface of the ATT–SnO_2. After vigorous stirring for 4 h, the suspension was filtered, washed with water, dried at 80 °C and calcined at 300 °C for 4 h. After grinding to about 200 meshes in a carnelian mortar, SnO_2–TiO_2 binary oxides coated on to ATT were obtained and labelled as ATT–SnO_2–TiO_2-*r*, where *r* represented the proportion of SnO_2 and TiO_2 loaded.

2.2. Characterization

The crystalline phase structure was determined with a ARL/X/TRA X-ray diffractometer using Cu Kα radiation. The BET surface area was evaluated by N_2 adsorption in a constant volume adsorption apparatus (Coulter SA 3100). Scanning electron micrographs (SEM) were recorded on a LEO-1530VP SEM microscope at 25 keV and the transmission electron microscopy (TEM) analysis was performed on a JEOL-2100 microscope, operating at 200 kV. The samples were dispersed in ethanol and treated with ultrasound for 5 min, and then deposited on a copper grid coated with a preformed hole-filled carbon film. The approximate content of the covered TiO_2 and SnO_2 was determined by inductively coupled plasma (ICP) spectroscopy (Perkin-Elmer Optima-2000 DV). Before the test, the ATT–SnO_2–TiO_2 was dissolved in a mixed solution of H_2SO_4/H_2O_2 (3:1), and then the sediment filtered. The resulting solution was diluted to give concentrations of Ti^{3+} and Sn^{4+} of about 50 ppm.

2.3. Adsorption/photocatalytic activity measurements

The photoreactivity of the composite catalyst was evaluated by measuring the methyl orange decomposition under UV irradiation using an XPA photochemical reactor (Nanjing Xujiang Factory of Electrical Engineering, Jiangsu, China). A 300 W high-pressure mercury lamp provided the irradiation. The initial concentration of methyl orange in the quartz reaction vessel was fixed at 20 mg/L (pH ≈ 5) with an as-prepared catalyst loading of 1 g/L. The reaction cell (400 mL) was bubbled with air at a flow rate of 20 mL/min. The extent of the methyl orange decomposition was determined by measuring the value of the absorbance at 465 nm using a UV-1100 spectrometer. The decomposition rate of methyl orange was calculated by the following formula:

$$\text{Decomposition rate} = \frac{A_0 - A}{A_0} \times 100\%$$

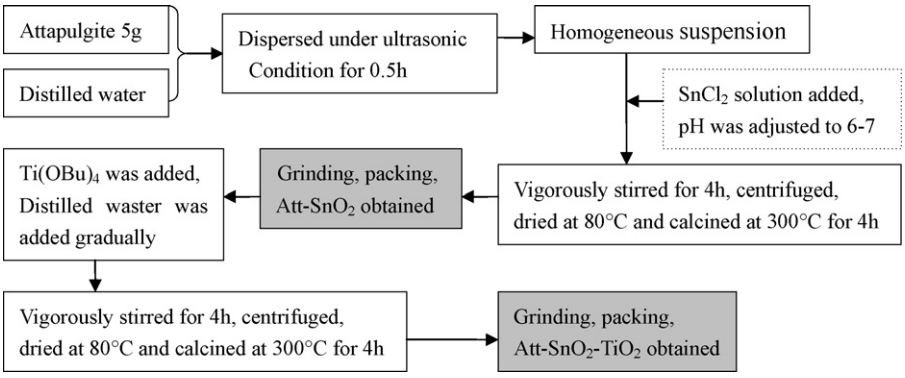

Fig. 1. Preparation procedure of ATT–SnO_2–TiO_2 composite photocatalyst.

where A_0 is the absorbance of the methyl orange solution before irradiation and A is the absorbance of methyl orange solution after irradiation.

For the repeated use of the photocatalysts, we accumulate the residual solution both in the reaction vessel and the centrifugal tubes. Then the residual solution was centrifuged, washed with distilled water, dried at 80 °C and activated at 300 °C for 4 h. The product obtained was labelled as ATT–SnO_2–TiO_2-*r* (callback). The photocatalytic property of ATT–SnO_2–TiO_2-*r* (callback) was measured under the same conditions as described above.

The adsorption capacity of the catalysts was measured in the similar way to that of photocatalytic activity measurements. The only difference is that the adsorption process was carried out without UV irradiation.

3. Results and discussion

3.1. Characterization of the ATT–SnO_2–TiO_2 nanocomposites

Fig. 2 shows the XRD patterns of the simple purified ATT powders before and after calcination for 4 h at 300 °C. The peak positions at 2θ values of 8.34°, 25.42°, 42.6° and 54.97° correspond to the crystal structure of ATT [34]. Low intensity scattering from other clay minerals such as montmorillonite and quartz were also found in the attapulgite. However, to be simple and operable, the ATT powder was used in the later sections without further purification because the tiny quantities of impurities clearly do not influence the properties of the composite photocatalyst. By comparing Fig. 2a with b, little difference is found between the scattering peaks from the two different samples, indicating that the crystal structure does not change after treatment at 300 °C. It is necessary to note that the ATT samples used in the following experiments were all calcined at 300 °C for 4 h.

Fig. 3 shows the XRD patterns of ATT–SnO_2–TiO_2 with different compositions. The characteristic reflections for ATT were observed in all of the samples (Fig. 3a–f). This phenomenon suggested that the modification process did not destroy the characteristic structure of ATT. In comparing the XRD patterns of ATT–SnO_2 (Fig. 3b) with that of ATT (Fig. 3a), the characteristic reflections for SnO_2 were also observed, indicating that SnO_2 particles had been loaded on to the surface of ATT [15,35]. The same reflections were detected in the XRD patterns of ATT–SnO_2–TiO_2 with different proportions [r = 0.25 and r = 0.5] (Fig. 3c and d), which were caused by the larger amounts of SnO_2 compared with those of TiO_2. The characteristic reflections for TiO_2 (anatase) appeared in the XRD patterns of ATT–SnO_2–TiO_2-0.75 (Fig. 3e) and the reflections for SnO_2 were also detected. From then on, the characteristic reflections of TiO_2 strengthened and the reflections of SnO_2 weakened gradually, with increasing amounts of TiO_2 (Fig. 3f and g). All these results implied that the SnO_2–TiO_2 binary oxides were loaded on to the surface of the ATT. The different dosages $r = n_{Ti}/(n_{Ti} + n_{Sn})$ have an effect on the crystallogram of ATT–SnO_2–TiO_2; the more TiO_2 was added, the higher would be the intensities of the TiO_2 reflections. Accordingly, this result may influence the photocalytic property of ATT–SnO_2–TiO_2 with different proportions of SnO_2–TiO_2.

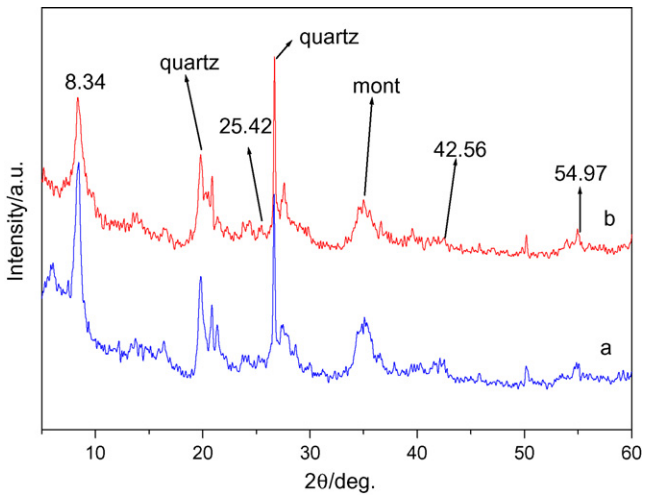

Fig. 2. XRD patterns of attapulgite (a) before and (b) after calcination at 300 °C.

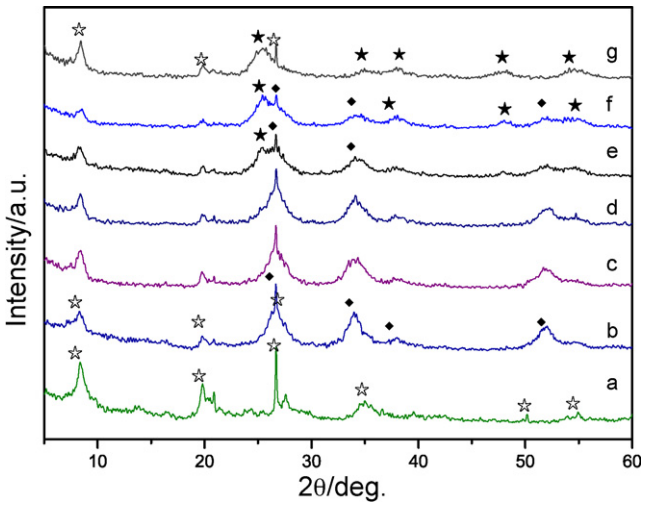

Fig. 3. XRD patterns of samples (a) ATT, (b) ATT–SnO_2-0.0, (c) ATT–SnO_2–TiO_2-0.25, (d) ATT–SnO_2–TiO_2-0.5, (e) ATT–SnO_2–TiO_2-0.75, (f) ATT–SnO_2–TiO_2-0.82, (g) ATT–TiO_2-1.0. (☆) attapulgite, (★) TiO_2 (anatase) and (⧫) SnO_2.

Fig. 4 shows the XRD patterns of ATT–SnO_2–TiO_2-0.82 before and after three photocatalysis runs. It can be seen that the XRD patterns were quite consistent with each other, indicating that the photocatalyst maintained its stable structure after being used three times as a catalyst. This result suggests that the ATT–SnO_2–TiO_2 composite catalyst can be used repeatedly.

Fig. 5 shows the TEM images of ATT and ATT–SnO_2–TiO_2-0.82. After simple purification, the ATT (Fig. 5a) emerged as rods (or fibers) and dispersed very well in water with an average diameter of about 20 nm and a length of 500–2000 nm. Fig. 5b is the TEM photograph of ATT–SnO_2–TiO_2-0.82. It demonstrates that the SnO_2–TiO_2 nanocomposites were loaded successfully on to the sur-

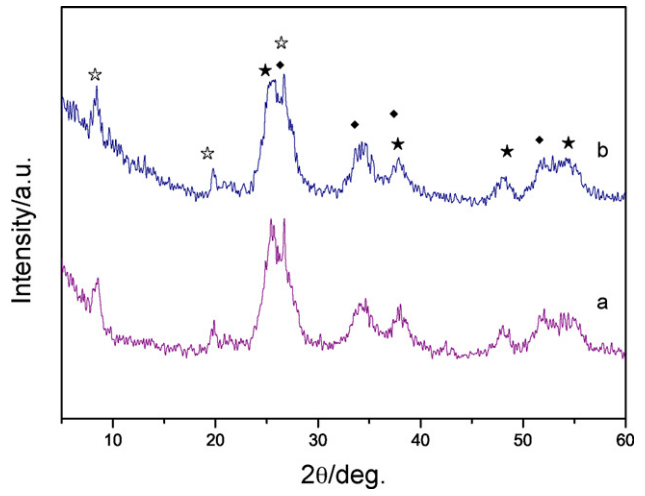

Fig. 4. XRD patterns of ATT–SnO_2–TiO_2-0.82 (a) before catalysis (b) after three times of catalysis. (☆) attapulgite, (★) TiO_2 (anatase) and (⧫) SnO_2.

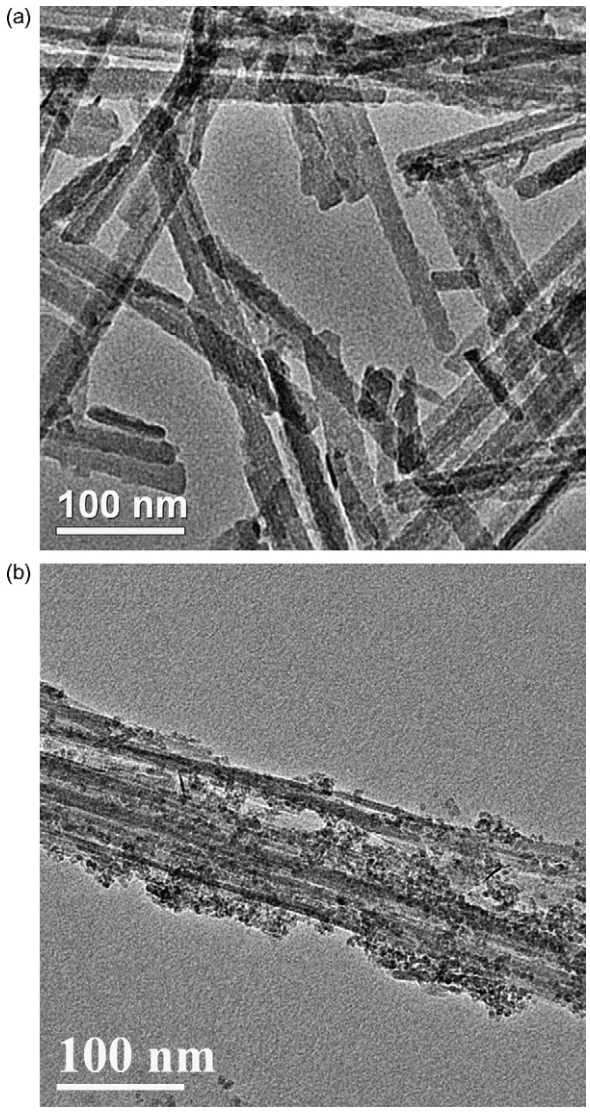

Fig. 5. TEM images of samples: (a) attapulgite (b) ATT–SnO_2–TiO_2-0.82.

face of ATT and their average particle size was about 10 nm. The sample shows a uniform distribution of spherical particles, without any obvious aggregation, dispersed over the surface of the ATT fibers. TEM images of other ATT–SnO_2–TiO_2 (r = 0.0, 0.25, 0.33, 0.50, 0.67, 0.75, 0.80, 0.86, 1.0) nanocomposites were quite similar.

The SEM images also confirmed the above result (Fig. 6). Comparing with the original ATT (Fig. 6a), the outer structure of ATT–SnO_2–TiO_2 (Fig. 6b) had obviously changed. Because the particles are somewhat damaged during their production, the average size of the ATT composites was reduced and the edges and corners of the ATT rods were no longer so sharp. At the same time, there are lots of ultrafine particles loaded on to the interface of the ATT. All these results directly demonstrate that the ATT–SnO_2–TiO_2 nanocomposites had been successfully synthesized.

The Ti or Sn content in the deposited photocatalysts was determined by ICP and the results are shown in Table 1. It can be seen that the content of Ti and Sn was slightly lower (about 4%) than the theoretical values because of the mass loss during the dissolving process. However, the molar ratio of Ti or Sn is consistent with the intended composition, from the quantities added to the reactor as raw material. This suggests that the composition of the composite catalysts can be controlled by *in situ* sol–gel techniques.

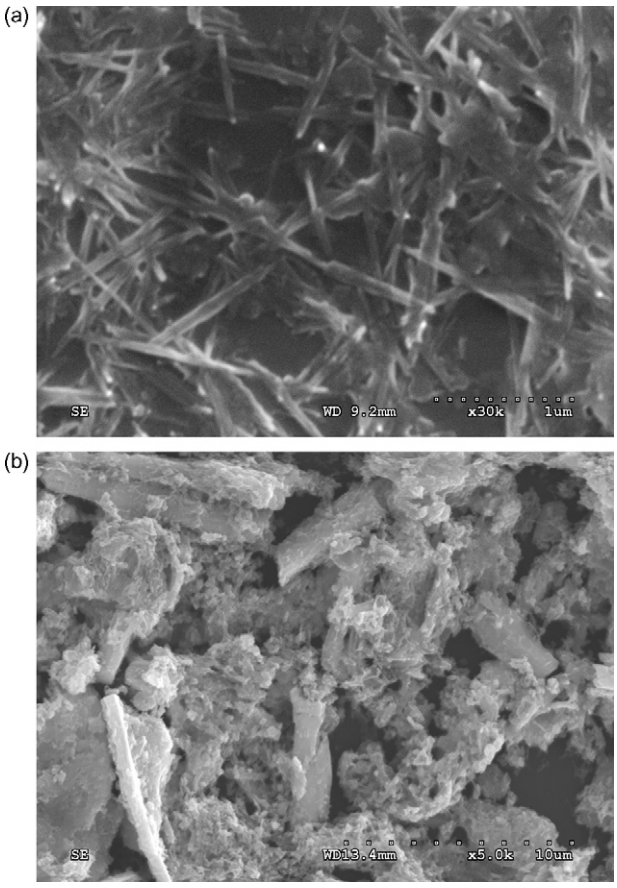

Fig. 6. SEM images of samples: (a) attapulgite and (b) ATT–SnO_2–TiO_2-0.82.

The nitrogen adsorption–desorption isotherms of ATT, ATT–SnO_2 and ATT–SnO_2–TiO_2 are shown in Fig. 7, and their BET surface area is listed in Table 1. In general, the surface area varies slightly before and after the coating modification (Table 1), indicating that the characteristic structure of ATT was maintained, which is consistent with the XRD and TEM results. The surface area of ATT–SnO_2–TiO_2 with different values of $r = n_{Ti}/(n_{Ti} + n_{Sn})$ changed in the sequence ATT–TiO_2 > ATT–SnO_2–TiO_2 > ATT–SnO_2. The pore volume and BET surface area of the ATT composites

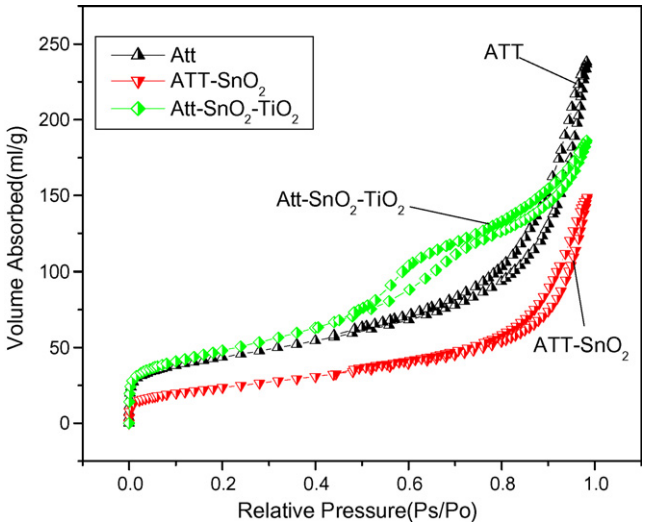

Fig. 7. N_2 sorption–desorption isotherms of ATT and other composite catalysts.

Table 1
Amount of Ti, Sn and specific surface area of the product.

Sample	ATT (300 °C)	ATT–SnO_2 (r = 0.0)	ATT–SnO_2–TiO_2 (r = 0.25)	ATT–SnO_2–TiO_2 (r = 0.82)	ATT–SnO_2–TiO_2 (r = 0.82)(callback)	ATT–TiO_2 (r = 1.0)
Content of Ti (wt.%)	0	0	2.34	16.14	16.09	8.26
Content of Sn (wt.%)	0	18.13	17.42	16.83	16.20	0
BET ($m^2\ g^{-1}$)	155.2	119.30	150.42	147.03	134.77	202.11

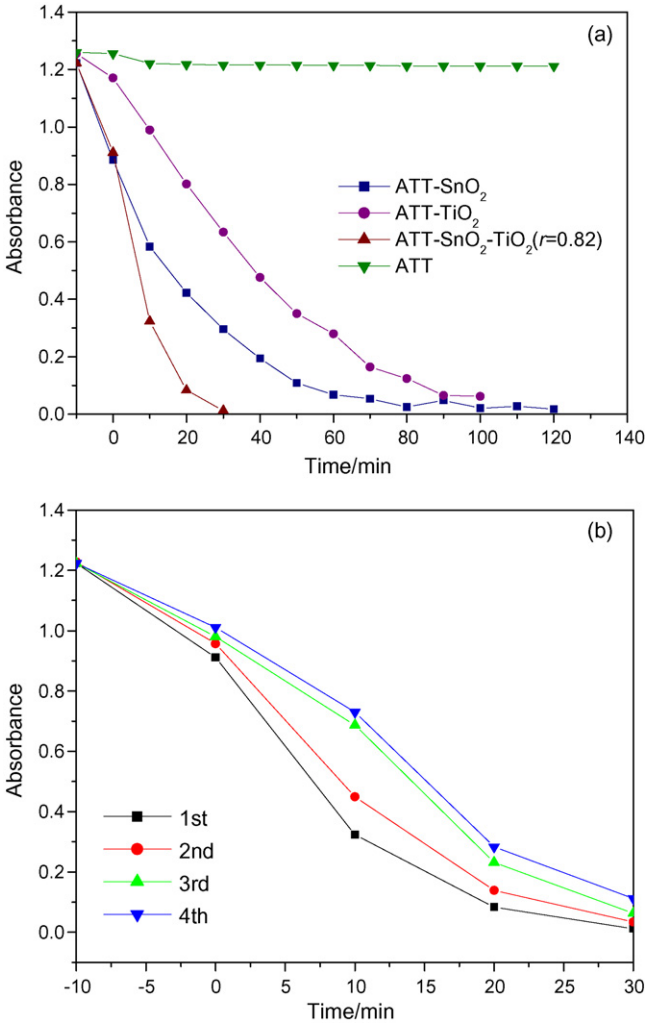

Fig. 8. Photocatalytic degradation of methyl orange by: (a) different catalyst and (b) ATT–SnO_2–TiO_2-0.82 (callback).

decreased slightly when SnO_2 or SnO_2–TiO_2 binary oxides were deposited on it. This may be caused by the blockage of the ATT pores with nanosized particles. The BET surface area of ATT–SnO_2–TiO_2-0.82 (callback) is also presented and shows a modest decrease after usage for photocatalysis three times, suggesting the stability over repeated usage of the photocatalyst. On the other hand, the isotherm profiles of ATT and ATT–SnO_2 were classified as type III, and the profile of ATT–SnO_2–TiO_2 was classified as type IV, according to the IUPAC classification [8]. The different isotherm profiles of type III and type IV of the samples indicated different microporous structures. This difference could affect their catalytic performance significantly.

3.2. Adsorption/photocatalytic properties of attapulgite–SnO_2–TiO_2 nanocomposites

The photocatalytic activities of a series of photocatalysts were characterized by the degradation test of methyl orange with UV irradiation (Fig. 8 and Table 2). According to the blank test, the original ATT did not possess any photocatalytic activity on methyl orange and the faint decrease of absorbency (*ca.* 3%) was attributed to its poor adsorption and the degradation by UV irradiation. Since ATT carries a negative charge on its surface and the methyl orange molecule usually also carries a negative charge in solution (pH = 5–6), the sorption between ATT and methyl orange molecule was quite weak even though the ATT presents a high surface area. Hence, the adsorption or photocatalytic activity of composite photocatalysts resulted from the surface active oxides.

As shown in Fig. 8a, the order of photocatalytic activity for the degradation of methyl orange was as follows: ATT–SnO_2–TiO_2 > ATT–SnO_2 > ATT–TiO_2. The photocatalytic activity of ATT–SnO_2 was better than that of ATT–TiO_2, which may be caused by the higher adsorptive ability of ATT–SnO_2 (see Table 2). Since the surface SnO_2 presents acidic properties, it changes the composite catalyst surface charge from negative to positive; this is very helpful for the absorption of more methyl orange molecules on to the surface of the nanocomposites, allowing the photocatalyst to work efficiently (see Table 2). In contrast, the TiO_2 surface is almost neutral because the reaction solution pH is close to $pH_{zpc} \approx 6.8$ [36,37]. So the ATT–TiO_2 composite catalyst failed to absorb more methyl orange molecules even though it had a higher surface area. The excellent photocatalytic activity of ATT–SnO_2–TiO_2 nanocomposites should be attributed to its anatase structure as well as the sensitization by coupling with SnO_2. The different conduction bands of SnO_2 and TiO_2 result in the efficient separation of photoinduced electron–hole pairs and high quantum yield was achieved [8,9]. Also, its high specific surface area, good dispersibility and finer absorptive ability is very helpful for achieving better photoactivity. On the other hand, the different microporous structures may also be responsible for this result.

By comparing the photocatalytic activity of ATT–SnO_2–TiO_2-0.82 (callback) with that of ATT–SnO_2–TiO_2-0.82 (Fig. 8b), it was found that the photodecomposition rate of methyl orange decreased slightly, indicating that the ATT–SnO_2–TiO_2 could be reused.

Investigation of the photocatalytic activity of ATT–SnO_2–TiO_2 with different proportions of n_{Ti} and n_{Sn} (Table 2 and Fig. 9) shows that the photodecomposition rate of methyl orange increased with increasing TiO_2 content for all values of $r \leq 0.82$ and then decreased for $r > 0.82$. The highest degradation rate was reached by using

Table 2
Absorption and photodecomposition rate of methyl orange by different catalyst within 30 min.

Samples	ATT	ATT–SnO_2–TiO_2-r									
		0.0	0.25	0.33	0.50	0.67	0.75	0.8	0.82	0.86	1.0
Absorption (%)	0.74	46.92	11.71	7.03	20.52	19.62	23.33	28.04	38.85	29.07	2.91
Removal rate of methyl orange (%)	3.80	76	36	54	78	92	97	95	99	93	50

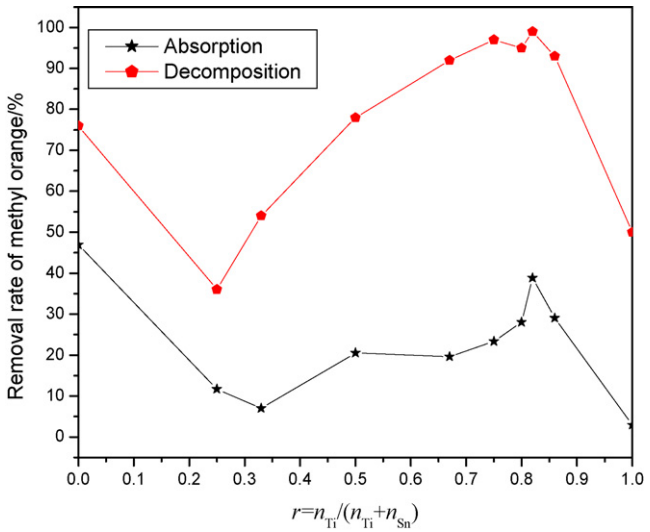

Fig. 9. Correlative chart of absorption and photodecomposition rate of methyl orange and $r = n_{Ti}/(n_{Ti} + n_{Sn})$.

ATT–SnO_2–TiO_2 ($r = 0.82$), which was 99% within 30 min. One possible reason for this phenomenon is that the absorption capacity of ATT–SnO_2–TiO_2 influences its photocatalytic activity. Generally, the higher the absorption capacity, the better the photocatalytic activity of the composite catalyst would be (see Table 2 and Fig. 9). At the same time, the amount of SnO_2 has a pronounced effect on the band structure of the composite catalyst obtained. The best photocatalyst is achieved when the ratio of SnO_2 and TiO_2 is adjusted to $r = n_{Ti}/(n_{Ti} + n_{Sn}) = 0.82$. A similar result has been found for other composite photocatalytic systems. Khan and Kim [38], Yang et al. [8] and El-Maghraby [9] also reported that the proportion of SnO_2 and TiO_2 affects the photocatalytic activity of TiO_2–SnO_2 composite catalysts. From Fig. 9, the ratio of SnO_2 and TiO_2 should be adjusted to $r = 0.67$–0.86 in order to achieve a good photocatalyst.

4. Conclusions

Attapulgite was used as the sorbent and the carrier of the SnO_2–TiO_2 photocatalyst, and a series of SnO_2–TiO_2 [$r = n_{Ti}/(n_{Ti} + n_{Sn}) = 0.0$, 0.25, 0.33, 0.50, 0.67, 0.75, 0.80, 0.82, 0.86, 1.0] hybrid oxides were deposited on to its surface by an *in situ* sol–gel technique. The products obtained were characterized carefully and the results showed that the surface morphology of the original attapulgite was effectively reformed and the SnO_2–TiO_2 nanoparticles, of average size about 10 nm, were successfully introduced on to the surface of the ATT fibers without obvious aggregation. Photocatalytic removal of methyl orange was studied using a series of the ATT–SnO_2–TiO_2 composite photocatalysts. It was found that the photoactivity of ATT was clearly improved after the coating modification and that the proportion $r = n_{Ti}/(n_{Ti} + n_{Sn})$ had an important effect on the photocatalytic property. This decreased in the sequence ATT–SnO_2–TiO_2 > ATT–SnO_2 > ATT–TiO_2 > ATT. The best ATT–SnO_2–TiO_2 photocatalyst was obtained when the value of r was adjusted to 0.82. For this, a decomposition rate of methyl orange 99% within 30 min was achieved. Experiments proved that the ATT–SnO_2–TiO_2 composite photocatalyst could be used repeatedly.

Acknowledgments

The authors thank the Program for Impellent Industrialization program of College Research Achievement (JH08-31) and College Natural Science Foundation (07KJB430010) of Jiangsu Province, Postdoctoral Science Foundations of the Department of Education of China (20060400941) and Jiangsu Province (0602003A), Doctoral Foundation of Huaiyin Teachers College (07HSBS005), Jiangsu Higher Institutions Key Basic Research Projects of Natural Science (07KJA15012) and Technological Research Foundation of Huai'an City (HAG08072) for financial support.

References

[1] D.V. Kozlov, A.V. Vorontsov, Sulphuric acid and Pt treatment of the photocatalytically active titanium dioxide, J. Catal. 258 (2008) 87–94.
[2] T. Takata, K. Shinohara, A. Tanaka, M. Hara, J.N. Knodo, K. Domen, A highly active photocatalyst for overall water splitting with a hydrated layered perovskites structure, J. Photochem. Photobiol. A: Chem. 106 (1997) 45–49.
[3] K. Tetsuy, G.Q. Gu, M. Yuuki, et al., Photocatalytic hydrogen production from water over a $LaMnO_3$/CdS nanocomposites prepared by the reverse micelle method, J. Mater. Chem. 13 (2003) 1186–1191.
[4] L.H. Zhang, P.J. Li, Z.Q. Gong, X.M. Li, Photocatalytic degradation of polycyclic aromatic hydrocarbons on soil surfaces using TiO_2 under UV light, J. Hazard. Mater. 158 (2008) 478–484.
[5] A. Fujishima, K. Honda, Electrochemical photocatalysis of water at a semiconductor electrode, Nature 37 (1972) 238.
[6] M.H. Zhou, J.G. Yu, S.W. Liu, P.C. Zhai, L. Jiang, Effects of calcination temperatures on photocatalytic activity of SnO_2/TiO_2 composite films prepared by an EPD method, J. Hazard. Mater. 154 (2008) 1141–1148.
[7] J.G. Yu, M.H.X. Zhou, B. Cheng, X.J. Zhao, Preparation, characterization and photocatalytic activity of in situ N, S-codoped TiO_2 powders, J. Mol. Catal. A: Chem. 246 (2006) 176–184.
[8] J. Yang, D. Li, X. Wang, et al., Rapid synthesis of nanocrystalline TiO_2/SnO_2 binary oxides and their photoinduced decomposition of methyl orange, J. Solid State Chem. 165 (2002) 193–198.
[9] E.M. El-Maghraby, Y. Nakamura, S. Rengakuji, Composite TiO_2–SnO_2 nanostructured films prepared by spin-coating with high photocatalytic performance, Catal. Commun. 9 (2008) 2357–2360.
[10] H. Tada, A. Hattori, Y. Tokihisa, K. Imai, N. Tohge, S. Ito, A patterned-TiO_2/SnO_2 bilayer type photocatalyst, J. Phys. Chem. B 104 (2000) 4585–4587.
[11] A. Hattori, Y. Tokihisa, H. Tada, N. Tohge, S. Ito, K. Hongo, R. Shiratsuchi, G. Nogami, Patterning effect of a sol–gel TiO_2 overlayer on the photocatalytic of a TiO_2/SnO_2bilayer-type photocatalyst, J. Sol–Gel Sci. Technol. 22 (2001) 53–58.
[12] T. Kawahara, Y. Konishi, H. Tada, N. Tohge, S. Ito, Patterned TiO_2/SnO_2 bilayer type photocatalyst. 2. Efficient dehydrogenation of methanol, Langmuir 17 (2001) 7442–7445.
[13] H. Tada, Y. Konishi, A. Kokubu, S. Ito, Patterned TiO_2/SnO_2 bilayer type photocatalyst. 3. Preferential deposition of Pt particles on the SnO_2 underlayer and its effect on photocatalytic activity, Langmuir 20 (2004) 3816–3819.
[14] K. Vinodgopal, P.V. Kamat, Enhanced rates of photocatalytic degradation of an azo-dye using TiO_2/SnO_2 coupled semiconductor thin films, Environ. Sci. Technol. 29 (1995) 841–845.
[15] J.J. Liu, X.P. Li, S.L. Zuo, Y.C. Yu, Preparation and photocatalytic activity of silver and TiO_2 nanoparticles/montmorillonite composites, Appl. Clay Sci. 37 (2007) 275–280.
[16] T. Torimoto, S. Ito, S. Kuwabata, H. Yoneyama, Effects of adsorbents used as supports for titanium dioxide loading on photocatalytic degradation of propyzamide, Environ. Sci. Technol. 30 (1996) 1275–1281.
[17] J. Matos, J. Laine, J.M. Herrmann, Effect of the type of activated carbons on the photocatalytic defradation of aqueous organic pollutants by UV-irradiated titania, J. Catal. 200 (2001) 10–20.
[18] Z.Q. Lei, Q.H. Zhang, R.M. Wang, G.F. Ma, C.G. Jia, Clean and selective Baeyer–Villiger oxidation of ketones with hydrogen peroxide catalyzed by Sn-palygorskite, J. Organomet. Chem. 26 (2006) 5767–5773.
[19] P. Liu, T.M. Wang, Adsorption properties of hyperbranched aliphatic polyester grafted attapulgite towards heavy metal ions, J. Hazard. Mater. 149 (2007) 75–79.
[20] X.L. Guo, Y.D. Yao, G.F. Yin, Y.Q. Kang, Y. Luo, L. Zhuo, Preparation of decolorizing ceramsites for printing and dyeing wastewater with acid and base treated clay, Appl. Clay Sci. 40 (2008) 20–26.
[21] K. Shimizu, T. Kaneko, T. Fujishima, T. Kodama, H. Yoshida, Y. Kitayama, Selective oxidation of liquid hydrocarbons over photoirradiated TiO_2 pillared clays, Appl. Catal. A 225 (2002) 185–191.
[22] C. Ooka, H. Yoshida, M. Horio, K. Suzuki, T. Hattori, Adsorptive and photocatalytic performance of TiO_2 pillared montmorillonite in degradation of endocrine disruptors having different hydrophobicity, Appl. Catal. B: Environ. 41 (2003) 313–321.
[23] C. Ooka, H. Yoshida, M. Horio, K. Suzuki, T. Hattori, Highly hydrophobic TiO_2 pillared clay for photocatalytic degradation of organic compounds in water, Micropor. Mesopor. Mater. 67 (2004) 143–150.
[24] K. Mogyorosi, I. Dekany, J.H. Fendler, Preparation and characterization of clay mineral intercalated titanium dioxide nanoparticles, Langmuir 19 (2003) 2938–2946.
[25] L. Korosi, R. Mogyorosi, R. Kun, J. Nemeth, I. Dékány, Preparation and photooxidation properties of metal oxide semiconductor incorporated in layer silicates, Prog. Colloid Polym. Sci. 125 (2004) 27–33.

[26] J.L. Cao, G.S. Shao, Y. Wang, Y.P. Liu, Z.Y. Yuan, CuO catalysts supported on attapulgite clay for low-temperature CO oxidation, Catal. Commun. 9 (2008) 2555–2559.
[27] H. Chen, A. Wang, Kinetic and isothermal studies of lead ion adsorption onto palygorskite clay, J. Colloid Interf. Sci. 307 (2007) 309–316.
[28] J. Huang, Y. Liu, Y. Liu, X. Wang, Effect of attapulgite pore size distribution on soybean oil bleaching, J. Am. Oil Chem. Soc. 84 (2007) 687–692.
[29] D. Zhao, J. Zhao, N. Liu, Surface characteristics and photoactivity of silver-modified palygorskite clays coated with nanosized titanium dioxide particles, Mater. Charact. 58 (2007) 249–255.
[30] D.M.A. Melo, J.A.C. Ruiz, M.A.F. Melo, E.V. Sobrinho, A.E. Martinelli, Preparation and characterization of lanthanum palygorskite clays as acid catalysts, J. Alloy Compd. 344 (2002) 352–355.
[31] S. Miao, Z. Liu, Z. Zhang, B. Han, Z. Miao, K. Ding, G. An, Ionic liquid-assisted immobilization of rh on attapulgite and its application in cyclohexene hydrogenation, J. Phys. Chem. C 111 (2007) 2185–2190.
[32] D. Zhao, J. Zhou, N. Liu, Characterization of the structure and catalytic activity of copper modified palygorskite/TiO_2 (Cu^{2+}–PG/TiO_2) catalysts, Mater. Sci. Eng. A 431 (2006) 256–262.
[33] D.M.A. Melo, J.A.C. Ruiz, M.A.F. Melo, E.V. Sobrinho, M. Schmall, Preparation and characterization of terbium palygorskite clay as acid catalyst, Micropor. Mesopor. Mater. 38 (2000) 345–349.
[34] W.S. Wu, Q.H. Fan, J.Z. Xu, et al., Sorption–desorption of Th (IV) on attapulgite: Effects of pH, ionic strength and temperature, Appl. Radiat. Isotopes 65 (2007) 1108–1114.
[35] X.Y. Hu, T.C. Zhang, Z. Jin, J.X. Zhang, et al., Fabrication of carbon-modified TiO_2 nanotube arrays and their photocatalytic activity, Mater. Lett. 62 (2008) 4579–4581.
[36] R. Vargas, O. Núñez, Hydrogen bond interactions at the TiO_2 surface: their contribution to the pH dependent photo-catalytic degradation of *p*-nitrophenol, J. Mol. Catal. A: Chem. 300 (2009) 65–71.
[37] A. Neren Ökte, Ö. Yılmaz, Photodecolorization of methyl orange by yttrium incorporated TiO_2 supported ZSM-5, Appl. Catal. B: Environ. 85 (2008) 92–102.
[38] R. Khan, T.-J. Kim, Preparation and application of visible-light-responsive Ni-doped and SnO_2-coupled TiO_2 nanocomposite photocatalysts, J. Hazard. Mater. 163 (2009) 1179–1184.